

## Observation of currents in Karun River

Maziar Khosravi<sup>1,\*</sup>, Seyed Mostafa Siadatmousavi<sup>2</sup>, Sadegh Yari<sup>1</sup>, and Jafar Azizpour<sup>1</sup>

<sup>1</sup> Iranian National Institute for Oceanography and Atmospheric Sciences, Tehran, Iran

<sup>2</sup> Iran University of Science and Technology, Tehran, Iran

*Received: 2016-11-30      Accepted: 2017-01-11*

### Abstract

This paper represents the results of Karun river field measurements during one month in spring, 2013. This measurement was conducted on the currents in a location with an average depth of 5 meters and a distance of approximately 120 km from the northern end of the Persian Gulf, in order to better understanding the currents' hydrodynamics. Spectral analysis of the currents showed a high magnitude of energy in tidal frequencies that expresses the effect of tides on these measurements. The results indicated that the maximum measured current by a current-meter was 70.6 cm/s, in a seaward direction, and unexpectedly corresponded with the neap tide. The high river discharge concurrently with the neap tide, cause this maximum velocity. In the observation period, the most important factors for determination of river flow direction were tides along with the river discharge variations. Moreover, it is noticeable that harmonic analysis of the sea surface level data, showed that  $M_2$ ,  $K_1$ ,  $O_1$  were the most important tidal frequencies with relative predominance of semidiurnal tides at the time and place of the measurement.

**Keywords:** Karun River; Currents; Tides; River Discharge.

### 1. Introduction

Karun River in Khuzestan province is the only navigable waterway and the largest river basin in Iran. Karun River with a length of 867 km and a basin area of 71,980 km<sup>2</sup> originated from Zard-Kuh in the Zagros Mountains and ultimately discharged in Arvand-Rud as a main source of fresh water in the Persian Gulf. Karun basin has three kinds of climate: the mountainous, foothills, and desert. Karun basin's climate fluctuates from a hot and dry condition in summer with temperatures higher than

50 °C to a cold winter with temperature less than zero. The total annual rainfall in this basin changes from 150 mm in plains to 1200 mm in mountainous (UN-ESCWA and BG, 2013).

Karun river discharge's variations can be due to water harvesting and dams' output changes during peak electricity consumption. Furthermore, monthly and natural flow regime in the Karun River is described with the maximum and dominant current of the melted water in the months of March and April and the minimum flow in September and October.

This paper is the first study in which represents

\* Corresponding Author: mazyar.khosravi2007@gmail.com

the long-term field measurement of Karun River currents. Measuring the currents was conducted by the current meter at geographical location of  $30^{\circ} 44' 37.65''$  N and  $48^{\circ} 24' 57.85''$  E, to describe the currents' hydrodynamics (Figure 1). Moreover, the current meter, has a pressure sensor, thus the water level fluctuations are recorded during the period in order to analyze and extract tidal components. Average water depth was about 5 meters and the current meter was vertically located at a depth of 2.5 meters above the riverbed. Distance of measurement's location to the northern end of Persian Gulf is 120 km. To better understanding of the Karun river current dynamics, the data of daily variations of Karun River discharge were investigated and analyzed in Farsiat station at  $30^{\circ} 59' 20''$  N  $48^{\circ} 22' 47''$  E, where is located in the upstream flow direction of the current-meter location. The data that corresponds to the 92-day period (from March 21 to June 20) obtained from the discharge data archived in Iran Water Resources Management Organization.

## 2. Materials and methods

Moorings are appropriate platforms for oceanographic instruments for long-term

measurements in a particular position. Moorings record their measurements using Eulerian method. Mooring designing depends on the water depth and the type of instruments used in the measurement, but in any case the basic components of an oceanographic mooring consists of an anchor, mooring lines (rope and chain), and one or more flotation buoy to have a vertical mooring line (Trask and Weller, 2009). The field operation was conducted in May 2013 by a mooring system. In this way, a Recorder Current Meter (RCM) was deployed in a depth of 2.5 meters above the Karun River seabed. In this mooring system, a weight of 100 kg as an anchor and a rope with a length of 2 meters as a connection between the RCM and the anchor were utilized. Moreover, a 42-kg flotation buoy was used to neuter the RCM's weight. The measurements performed for one month-length, from 09:00 of 29 April 2013 to 16:20 of 29 May 2013, with a time step of 20 minutes. Figure 2 illustrates a schematic of mooring components.

In addition, the considered time step was as enough to resolve the tide and current variations from the observed data. The current meter has an accuracy of 0.5 cm/s for measuring currents, and  $\pm 5$  degrees in the current direction. There were no system failure and battery discharge during the period of study and



Figure 1. Location of current measurements in Darkhovayn and Karun River discharge measurement in Farsiat station

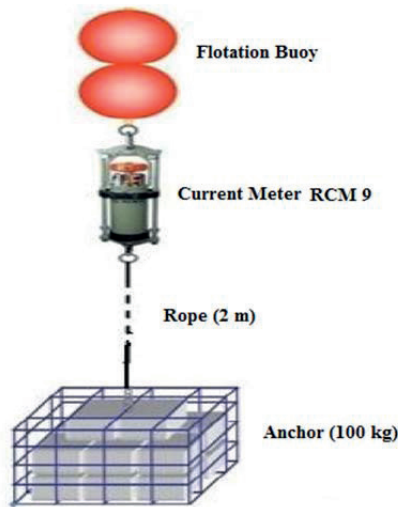


Figure 2. Mooring components

measurements. In addition, the difference between each data with its previous one was calculated. In this way, all unacceptable data removed and replaced with the proper reconstructed data.

### 2.1. Theory and Computation

The first step in analyzing the current data in this study was to calculate the current speed in along river direction (northeast-southwest) through the principal component analysis (Preisendorfer and

Mobley, 1988). Then, to understand the current hydrodynamics and to describe the forces in the region, the spectral analysis of time series data was used. In Fourier transformation equations, time series data are expressed by summation of Sine and Cosine functions. Using the horizontal components of velocity in Rotary Spectra, the energy is decomposed in two components in the case of rotating frequency; clockwise (CW) and counterclockwise (CCW) (Hayashi, 1979). In an identified frequency, if a component value is much larger than the other components, there will be a symmetrically round moving. In other words, if two components are equal at a particular frequency, moving will be on a straight line. Other cases between these two can be considered as an elliptical motion after the larger component. Furthermore, the separation of tidal signals of currents and then tidal current from other signals was made using harmonic analysis through the T- Tide package. In classical tidal analysis, the tidal signals are the summation of sinusoidal functions in the frequencies related to the astronomical parameters (Pawlowicz *et al.*, 2002). All calculations and provided codes are conducted in MATLAB.

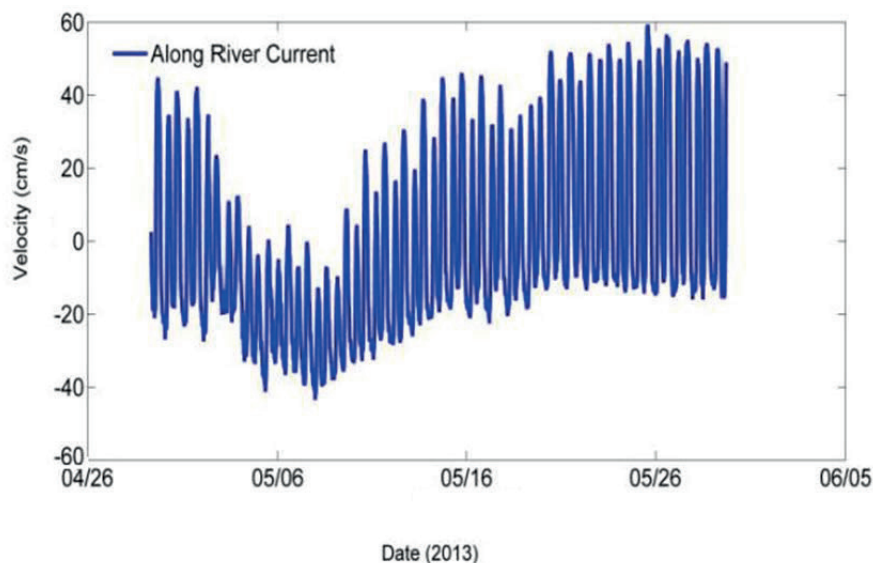


Figure 3. Changes of current velocity along the river in a depth of 2.5 meters above the riverbed in May 2013

### 3. Results and Discussion

Because of the long-length of Karun River (867 km), the results of the field measurement of currents have been limited to the place and time and cannot be generalized to the entire river or other seasons. Figures 3, 4, and 5 show the along river current's variations, tidal elevation, and the temperature recorded by RCM, respectively. The results of principal component analysis showed that along the river, the maximum velocity in downstream flow direction was 60 cm/s and the maximum velocity in

upstream flow direction was 43.5 cm/s (Figure 3). Figure 4 implies that the days 6 and 19 of May were coinciding with the neap tide and the days of 13 and 27 of May were coinciding with spring tide. The results of the measurements of temperature sensor in 2.5-m above the seabed indicates gradually enhancement of at least 23 °C to the maximum 28 °C during the observation period in May (Figure 5). Increasing of temperature is due to the change of seasons and the transition from spring to early summer. The along-river current variations showed a seaward current in the period of 1 to 11 of May

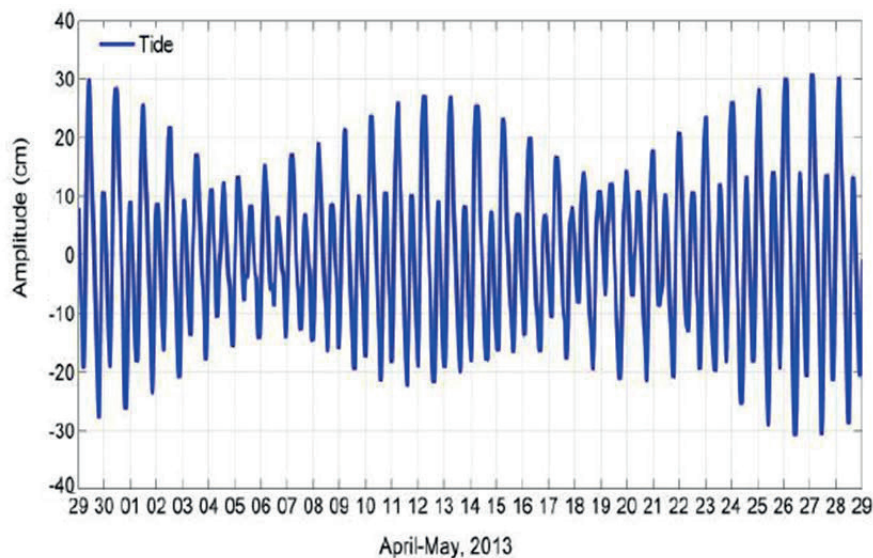


Figure 4. Tidal elevation variations (calculated from harmonic analysis on water level fluctuations)

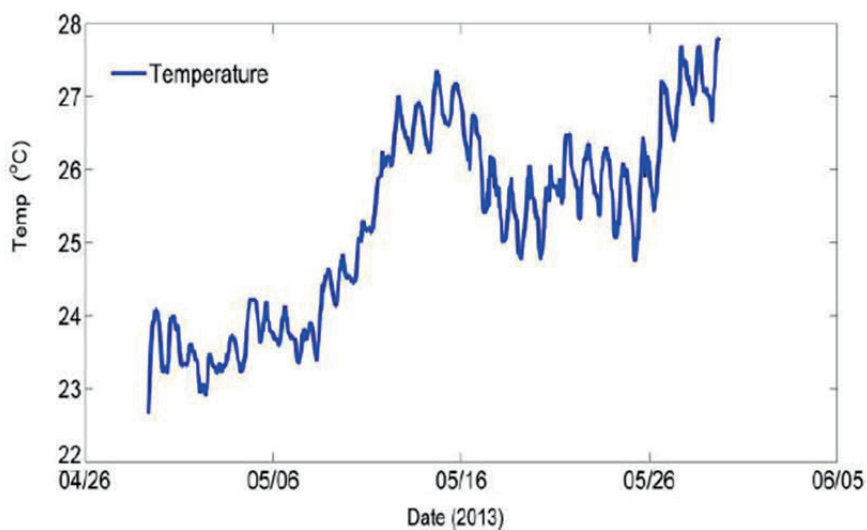


Figure 5. Temperature variations in a depth of 2.5 meters above the riverbed in May 2013

2013. Figure 6 shows that the Karun River discharge is typically less than  $300\text{m}^3/\text{s}$ , but it was higher during this period. It reached to the peak on May 7 with magnitude of  $453\text{m}^3/\text{s}$ . River discharge is calculated by multiplying the current velocity and the related area. The area is also computed by multiplying the river width and river depth. It is obvious that the river width is constant during the time because of the steep riversides, but the depth varies (water level fluctuations) due to the tides, river discharge changes, and atmospheric fluctuations. Thus, increasing the river discharge leads to an increase in current's velocity, and

dropping in water fluctuations level was due to the neap tide occurrence. These are observable in Figures 3, 6, and 8 that show the current velocity, river discharge, and current direction, respectively. In addition, Figure 8 shows the trend of water level fluctuations, which represents that the drop in water level fluctuations on 6-8th of May was coincided with neap tide.

In this period, at high river discharge, the current direction was always seaward and the discharge enhancement was overcome to the flood flow (Figures 3 and 7). The maximum current measured by the RCM on May 7 was coincided with high river

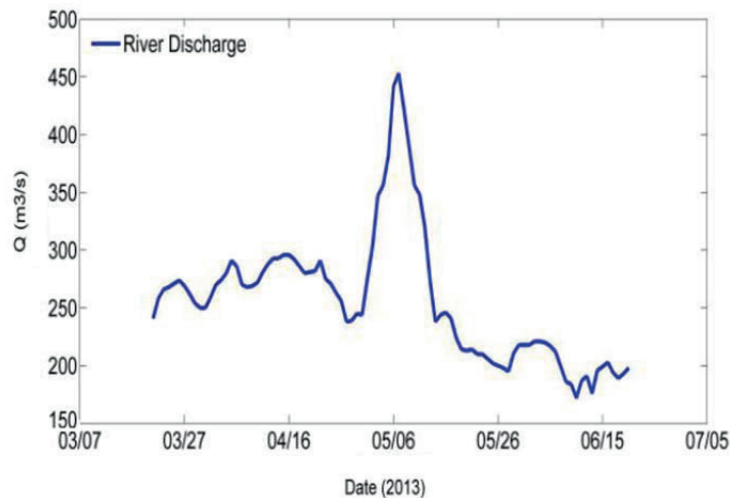


Figure 6. Changes in daily discharge of Karun River, Farsiat station

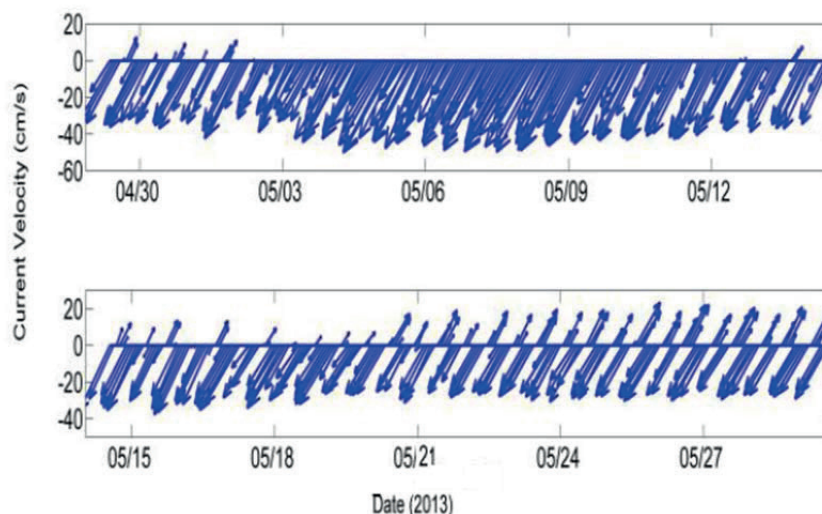


Figure 7. Stick-plot of Karun River flow, Darkhoein station

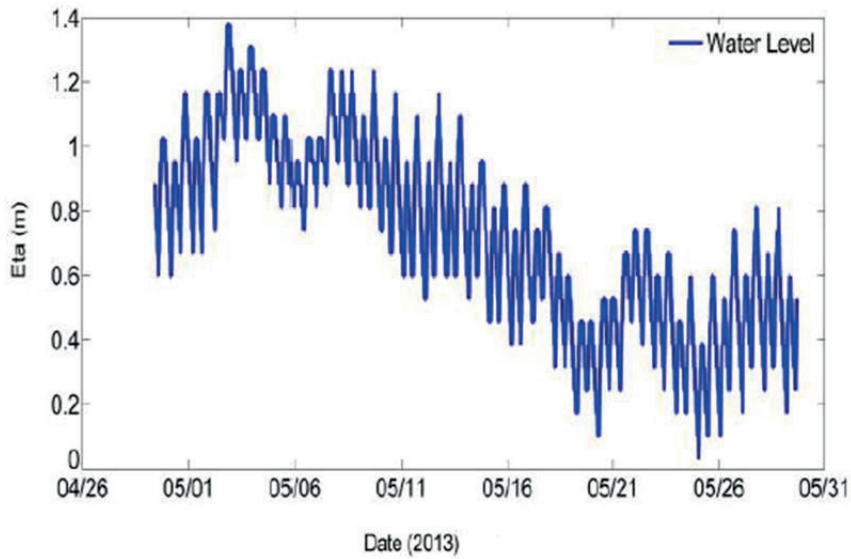


Figure 8. Water level fluctuations in Karun River, May 2013

discharge and it was 70.6 cm/s, in seaward direction and during neap tide despite the expectation was that the maximum current normally occurs during spring tide.

Table 1 represents the calculation of tidal amplitude and phase through the harmonic analysis on the Karun River water level fluctuations with 95% confidence interval estimates. As it is obvious in Table 1, the  $M_2$ ,  $K_1$ , and  $O_1$  are the most important tidal signals in the Karun River.

According to the Defant method, the ratio of tidal amplitude  $F$  is calculated by the following formula (Defant, 1961), and using the data in Table 1, its value obtained 0.7.

$$F = \frac{K_1 + O_1}{M_2 + S_2}$$

which represents a mixed semidiurnal tide in the Karun River. The result is in agreement with the calculated values from shallow and homogenous water models for the Persian Gulf (Figure 9). In fact, the tidal pattern in the northern Persian Gulf is mixed, and it changes from semidiurnal to diurnal tide. Thus, the tide in Karun River followed this pattern and the current measurements confirmed the mixed tide in this region. In other words, the tide in the Karun River is a combination of semidiurnal and diurnal signals with the relative predominance of semidiurnal signals.

Table 1. Amplitude and phase of tidal signals

Tidal signal	Frequency (cph)	Amplitude (m)	Amplitude error (m)	Phase (°)	Phase error (°)
M2	0.080511	0.135	0.01	142.25	4
K1	0.041781	0.079	0.005	57.89	4
O1	0.038731	0.042	0.005	35.88	8
S2	0.083333	0.038	0.01	201.96	15.6
MK3	0.122292	0.033	0.006	94.41	10.8

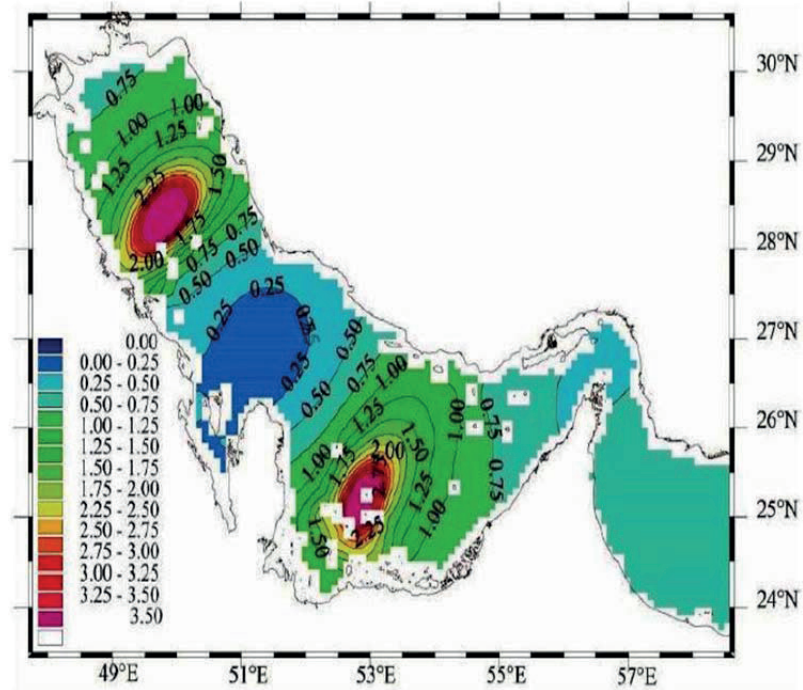


Figure 9. “F” parameter across the Persian Gulf indicates the type of tide (Pous *et al.*, 2012)

The results of spectral analysis on the current’s data at a depth of 2.5 meters above the riverbed during the study period indicates that with reduction in periodicity, the spectral energy drops in both directions, clockwise and counterclockwise (Figure 10). The wind mainly affects the lowest spectral energy in both CW and CCW directions and also at high frequency and low-periodicity.

In fact, the reason is the small river width, which does not allow a considerable momentum transfer to the water surface. Thus, the wind effect on current generation is negligible in the small river. The maximum spectral energy with frequency of 0.08 cph is observed in both directions; CW and CCW and is connected to the semidiurnal tide. Moreover, the maximum spectral energy at 0.041

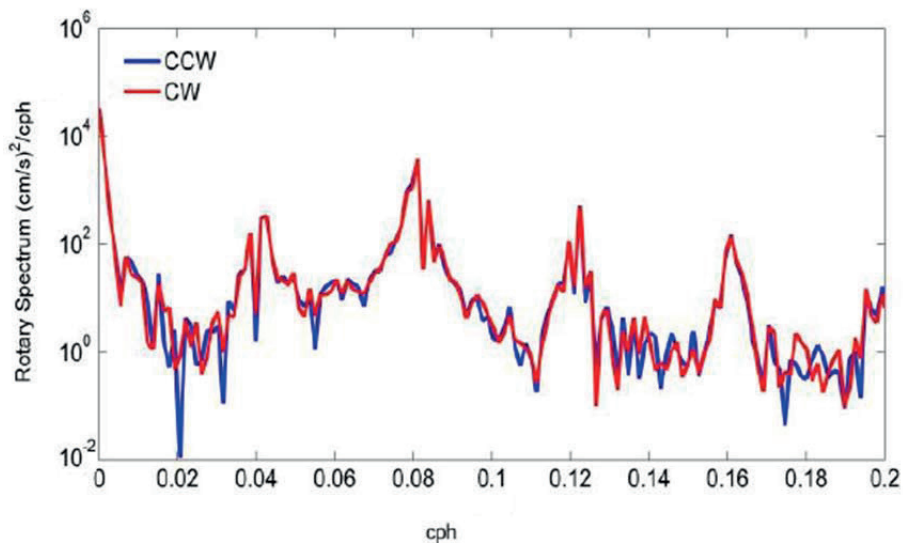


Figure 10. Spectral analysis for currents’ data along the Karun River in May 2013

cph frequency, in both CW and CCW directions, shows the relatively high energy in diurnal tides. Furthermore, two peaks with 0.121 cph and 0.161 cph were respectively connected to interactions of semidiurnal and diurnal tides and also semidiurnal harmonic tide. Thus, the figure illustrates that the tide has the high energy at low frequencies. As is obvious in Figure 10, the energy spectrum in both directions is almost symmetric. Therefore, because of the same energy in similar frequencies, the water mass movement is on a straight line that is consistent with water movement along the rivers.

Figure 11 compares three graphs of the general current, tidal current, and the residual current in the Karun River. The residual current was calculated by subtracting the river current from tidal current. Comparing the graphs it is clear that the river itself has a background energy that leads the river current into the sea. This energy can be due to a pressure gradient between the sea and the river caused by the river slope towards the sea, and the river discharge. The results of harmonic analysis indicate that the contribution of tidal current is 66.6% and so, the contribution of the residual current obtained 33.4%. However, as the spectral analysis results introduced the high-energy tides at low frequencies, herein it

introduces the tidal force as the dominant force in the area.

During the ebb flow, the tidal current along with the residual current flowed in the downstream direction and also during flood flow the tidal current with its high energy overcame to the residual current and flowed in upstream direction. Although, as stated from 1 to 11 May the current was always seaward because of high river discharge, and the tidal frequencies in the flood time did not have enough energy to change the current direction.

## Conclusions

This research introduced  $M_2$ ,  $K_1$ , and  $O_1$  as the most important tidal frequencies with the relative predominance of semidiurnal signal in Karun River during the period of observation. Typically, maximum current velocities were in spring tide, but unexpectedly, due to high river-discharge during 1-11 May, the maximum current velocity (70.6 cm/s) was on 7 May, seaward and concurrent with neap tide. Comparing the river current, tidal current, and residual current indicated an enhancement in the residual current coinciding with the neap tide, concurrent with the time of high river-discharge.

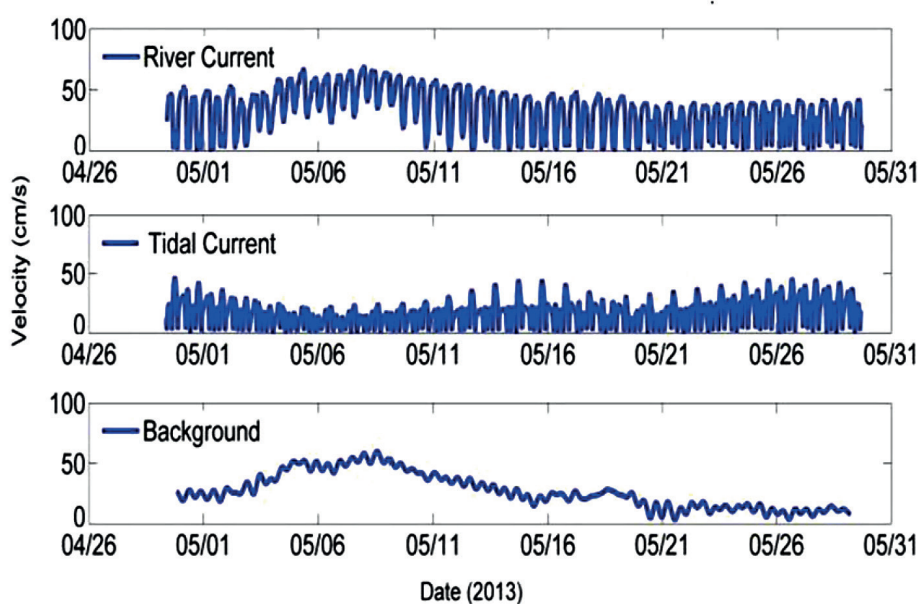


Figure 11. Comparing river current, tidal current, and residual current

Regardless of the period of 1 to 11 May when the current was seaward which river current overcomes on tidal frequencies and net current of river always generates a seaward movement in Karun River, tidal current velocities usually had higher values in comparison with the motion due to the residual current. Thus, it can be concluded that the river current in both directions of seaward and anti-seaward in an almost 120 km distance to the northern-end of the Persian Gulf, was highly affected by the tides. On the other hand, the tidal frequencies during the enhancement of river discharge were completely defeated by high velocities of river currents. Therefore, this study introduced not only the tidal frequencies but also the river discharge as the most important factors in determining the river current direction in the study area.

Resources in Western Asia, p. 147-167. New York: United Nations.

## References

- Defant, A. 1961. *Physical Oceanography*. London, UK: Macmillan.
- Hayashi, Y. 1979. Space-time spectral analysis of rotary vector series. *Journal of the atmospheric sciences*, 36(5):757-66.
- Pawlowicz, R., Beardsley, B., and Lentz, S. 2002. Classical tidal harmonic analysis including error estimates in MATLAB using T\_TIDE. *Computers & Geosciences*, 28(8): 929-937.
- Pous, S., Carton, X., and Lazure, P. 2012. A process study of the tidal circulation in the Persian Gulf. *Open Journal of Marine Science*, 2(4):131-140.
- Preisendorfer, R. W., and Mobley, C. D. 1988. *Principal component analysis in meteorology and oceanography*. Amsterdam: Elsevier.
- Trask, R. P., and Weller, R. A. 2009. Mooring, floats and current meters. In: Steele JH, Thorpe SA, Turekian KK, editors. *Measurement Techniques, Sensors and Platforms: Introduction*: Elsevier, 97-110.
- UN-ESCWA, and BG. 2013. *Shatt al Arab, Karkheh and Karun Rivers. Inventory of Shared Water*